

## MEASUREMENT AND THEORY OF TURBULENCE IN RR LYRAE

W. BENZ

Geneva Observatory; and Los Alamos National Laboratory

AND

R. F. STELLINGWERF

Mission Research Corporation

Received 1985 January 25; accepted 1985 March 18

## ABSTRACT

CORAVEL observations of time-dependent turbulence in RR Lyrae are presented. Variation in the width of the mean velocity correlation function implies turbulent velocities that peak at 5–10 km s<sup>-1</sup> for a brief interval of phase near minimum radius. Detailed comparison with a nonlinear pulsation model confirms the interpretation of broadening due to turbulence, since the modeled turbulent velocity agrees rather well in both amplitude and phasing with the observed velocities.

*Subject headings:* stars: pulsation — stars: RR Lyrae — turbulence

## I. INTRODUCTION

A classical problem in spectroscopy is the interpretation of “microturbulence” as derived from spectral line widths. The presence of contributing factors such as rotation, non-LTE effects, and many other potential line-broadening mechanisms makes quantitative determination of the turbulent velocity difficult. For variable stars, however, an additional factor may be used to analyze this problem: the time dependence of the convective velocity field. In this paper we present an initial attempt to apply this analysis to the surface turbulent velocities in RR Lyrae, using the sensitivity of the CORAVEL technique to estimate the turbulence, and invoking comparison with a nonlinear pulsation model to interpret the results.

## II. OBSERVATIONS

The observations of RR Lyrae-type stars add a serious problem to the usual difficulties of spectral line analysis: the short time scale during which the physical atmospheric parameters change. Any observational tool must have a high time resolution without losing precision. Currently, the best type of instrumentation corresponding to these criteria is the CORAVEL spectrovelocimeter (Baranne, Mayor, and Poncet 1979), which was initially developed to measure accurate radial velocities, but was also shown to provide high-precision rotational velocities (Benz and Mayor 1981, 1984). The integration time needed to make the measurements presented in this paper never exceeds about 4 minutes, which is 0.0055 of the pulsation period (0.567 days for RR Lyrae). We can therefore take the individual measurements as instantaneous values and neglect the broadening caused by the change of the radial velocity during the measurement.

The observations were made during two observing periods (1983 July and 1983 October) with the CORAVEL located at the 1 m Swiss telescope of the Observatoire de Haute-Provence, France. Let us recall in a few sentences the major characteristics of CORAVEL (for a complete description see Baranne, Mayor, and Poncet 1979). The spectrum of the measured star is cross-correlated with a mask located in the focal plane of the spectrograph. The cross-correlation function thus obtained can be considered as a “mean” of the 1500 spectral lines used. The signal-to-noise ratio is sufficiently high to accu-

rately analyze the pseudo-line profile down to a magnitude of about  $m_B = 11$  on a 1 m telescope. The data reduction consists of fitting a Gaussian to the points defining the measured signal. Three free parameters can be derived from the fit: the position of the minimum, the “ $\sigma$ ” [related to the half-width at half-maximum by  $\text{FWHM} = (2 \ln 2)^{0.5} \sigma$ ] and the cross-correlation area. These three parameters are directly related to the physical parameters: radial velocity, velocity field, and metallicity (Mayor 1980).

In the next section we present an analysis of the  $\sigma$  of the fitted Gaussian. We obtain the turbulent velocity from the width of the function in a way similar to the one adopted by Benz and Mayor (1982) in a study of Cepheids.

## III. DATA ANALYSIS

As mentioned above, the data were gathered during two observing periods. As each of these periods spans about 10 days, we will analyze each data set separately and neglect the small changes induced by the secondary (Blaschko) period of about 40 days. These changes may add some scatter to the mean curves but would in no way affect the conclusions of the present work.

## a) Radial Velocities

Figures 1a and 1b show the radial velocity curves for the two sets of observations. We will not discuss them in detail as they are going to be addressed elsewhere. For our purpose we nevertheless need to know what is the mean radial velocity of the star in order to correct the width of the correlation function for the broadening due to the geometrical effect. The difficulty here is that the velocity curve (as well as the light curve) is asymmetric with respect to the mean velocity of the star depending on the phase of the secondary period. The ideal would be to have observations covering entirely this secondary period; unfortunately, we here only have two points at different phase. We therefore have determined the mean velocity by taking into account only the parts of the radial velocity curves ranging between 0.–0.2 and 0.8–0.0. These parts are known to show little change due to the secondary period. By doing this we found a mean radial velocity of  $-74 \text{ km s}^{-1}$ . We also computed the mean velocity for both observing periods and we

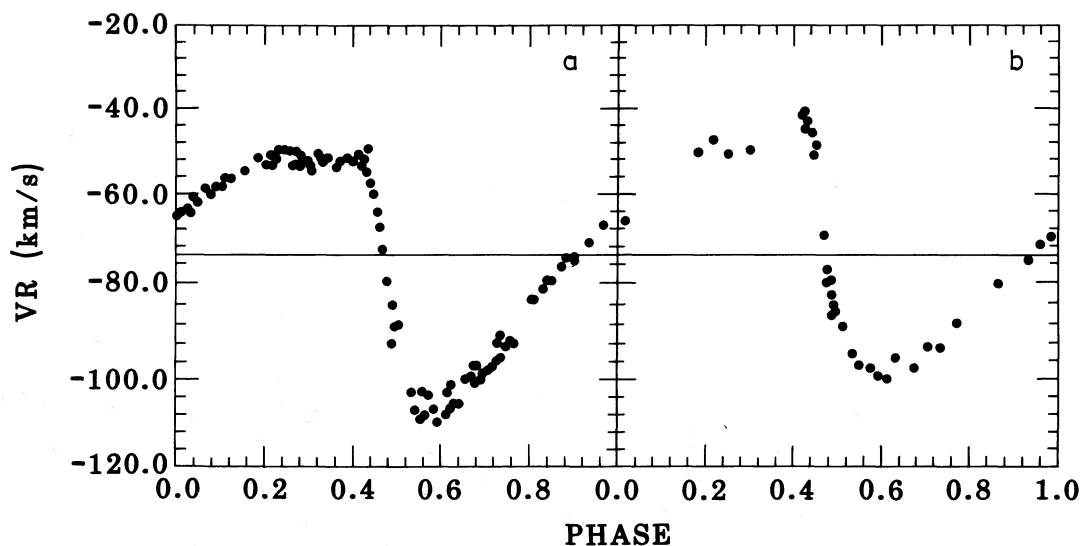


FIG. 1.—RR Lyrae radial velocity measurements vs. phase: (a) 1983 July; (b) 1983 October

found respectively  $-80 \text{ km s}^{-1}$  and  $-70 \text{ km s}^{-1}$ . This confirms the asymmetry of the radial velocity curve. The mean between these two numbers is  $-75 \text{ km s}^{-1}$ , which is rather close to the former estimation of the mean velocity. We therefore adopt as a mean velocity for RR Lyrae the value of  $-74 \pm 3 \text{ km s}^{-1}$ . Tests show that the exact value of the mean velocity does not affect the increase of the turbulent velocity near minimum radius. The adopted mean velocity is also plotted in Figures 1a and 1b.

#### b) Turbulent Velocities

Before deriving the turbulent velocity variations, we would like to briefly emphasize that the term "turbulence" here may not be hydrodynamic turbulence as characterized by an energy flow through eddies in the usual Kolmogoroff picture. We use here the definition used by the spectroscopists of the turbulence. This means that we identify all broadening mechanisms that are not rotation as "turbulence." This is a crude approximation since this broadening excess may include many effects

such as convection, magnetic fields, turbulence, etc., and mixes them in a single parameter. Nevertheless we will show that in the case studied here this broadening excess can be identified as being a measure of convective velocities.

Let us now consider the turbulent velocity as a function of pulsation phase. Figure 2a and 2b show the variation of the cross-correlation width ( $\sigma$ ) as a function of the phase (the phasing is the same as in the radial velocity curves). We first see that the width always exceeds the instrumental profile of CORAVEL, which is about  $6.7 \text{ km s}^{-1}$ . This difference may be interpreted as either rotation or as a remaining velocity field. For the present analysis, the interpretation of this effect is not important, since we are concerned only with the variation with phase of this quantity. We therefore take as the origin the minimum width measured during the whole period. It is interesting to note that this minimum width is achieved at the phase of maximum radius. This was previously noted by Benz and Mayor (1982) in their study of Cepheids. We will show below that maximum radius also corresponds to the phase of

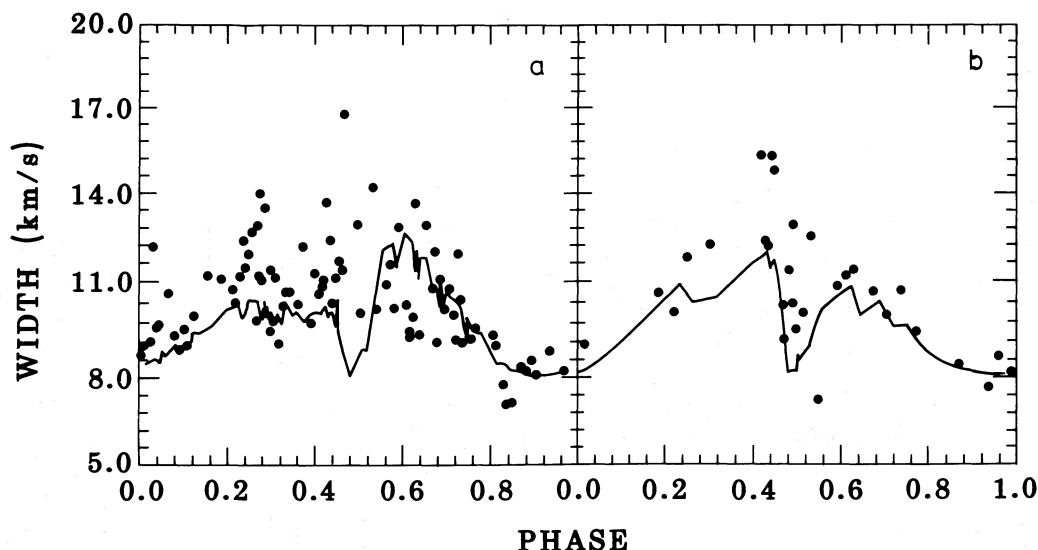


FIG. 2.—Width of the correlation function vs. phase for the two observing periods. Solid line: computed geometrical broadening using radial velocity data.

minimum convective velocities. The numerical value of the minimum width was taken to be  $8 \text{ km s}^{-1}$ . This value was then subtracted quadratically from all the measured widths. The remaining variations are interpreted as (1) broadening caused by the geometrical (projection) effect of the pulsation and (2) velocity field variations. To remove the geometrical effect we proceed as described in Benz and Mayor (1982). We will now summarize this procedure.

We compute a synthetic cross-correlation function at each point of phase by integrating over the surface of the star taking into account the limb darkening, instrumental profile, and energy distribution of the star and by imposing that the obtained radial velocity is equal to the observed one. After doing this we now have for each CORAVEL measurement a synthetic cross-correlation function having the same radial velocity but a width determined only by the geometrical broadening effect.

Let us call the observed width of the cross correlation function  $\sigma_{\text{obs}}$  and the synthetic width  $\sigma_{\text{syn}}$ . The broadening excess is easily computed using a quadratic difference and will be noted  $\sigma_{\text{turb}}$ .

$$\sigma_{\text{turb}} = \pm(|\sigma_{\text{obs}}^2 - \sigma_{\text{syn}}^2|)^{1/2}. \quad (1)$$

The  $\pm$  sign is determined by the sign of the differences of the  $\sigma$ 's. A negative  $\sigma_{\text{turb}}$  means that the observed width is smaller than the width obtained by taking only the geometrical effect into account. Obviously this should never be the case as there is no effect that could make spectral lines narrower. We show in the next paragraph that this fact may be easily interpreted as resulting from the photon noise on the cross-correlation. Figure 3a and 3b are plots of  $\sigma_{\text{turb}}$  as a function of phase with the same phasing as in the other figures. Before comparing these observations to theoretical models of RR Lyrae (see next section) we will discuss briefly the scatter of the computed  $\sigma_{\text{turb}}$ .

The mask of CORAVEL is an image of the spectrum of Arcturus, which is a K2 giant. It is based mainly (80%) on iron lines (Fe I and Fe II), which are common in the spectrum of late-type stars. The spectral range of stars measurable by CORAVEL consequently extends from approximately F5 to the coolest stars. The upper limit is further limited by the

contrast of the function. If the contrast falls below 2%, the measure becomes uncertain. One cause of lower contrast would be a high rate of rotation. For RR Lyrae the contrast of the cross-correlation function is near the critical value of 2%—not because the star rotates too fast, but because the spectral type of RR Lyrae is located just at the edge of the measurable domain. This makes the observations difficult and means that they are affected by higher uncertainties than the usual measurements of CORAVEL. To explain how the width of the cross-correlation function might be affected by photon noise, we made a set of simple simulations. We take a Gaussian having the same parameters (width, contrast) as the RR Lyrae case. We then add to this Gaussian a random noise whose amplitude is given by the square root of the number of photons defining the measured signal. We then compute the reduction as for the observations. The same procedure is repeated 100 times. We find that a dispersion around the mean width is as great as  $1.1 \text{ km s}^{-1}$ . This means that one could have up to about  $3 \text{ km s}^{-1}$  scatter around the mean width because of photon noise. In examining Figure 3 one should keep in mind this order of magnitude. It explains clearly why the observed width is sometimes smaller than the one computed from the geometrical effect. It also clearly shows that the high velocities derived around minimum radius could not be explained by photon noise. We will show in the next section that the origin of these high velocities most likely lies in the increase of convective velocities near minimum radius.

#### IV. MODEL RESULTS

Although it is probably true that a completely satisfactory theoretical treatment of the coupled convection/pulsation does not yet exist, much progress toward a workable solution has been made in recent years. The CORAVEL observations discussed in this paper represent one of the very few direct observational tests of such a theory, especially since the phase dependence of the observed turbulence should be reflected in the time dependence of the convection theory. In addition, if the theory is sound, a more accurate interpretation of the observational data should be possible.

In this section a comparison is made with a recently published fully convective RR Lyrae model. The model is

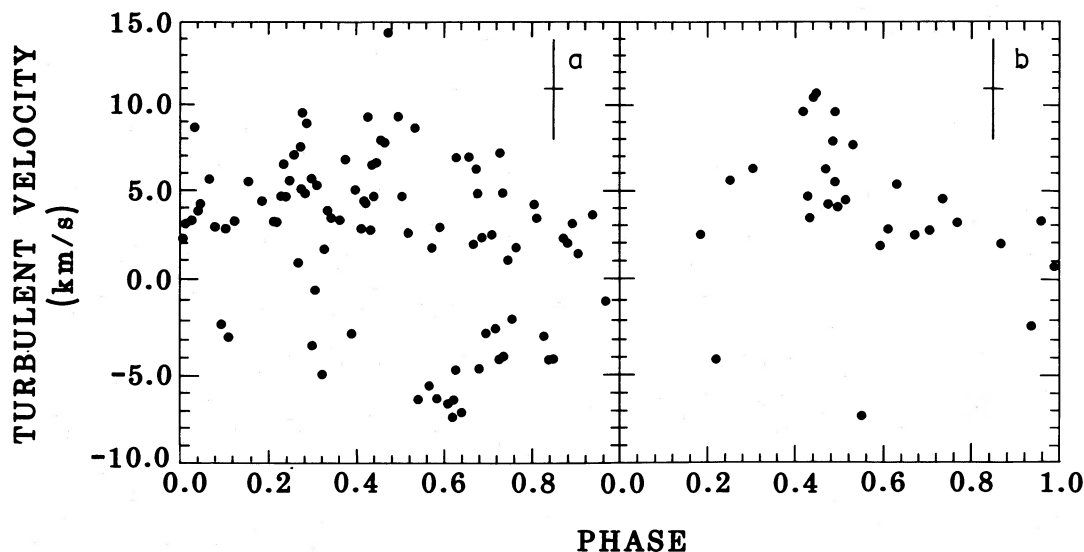


FIG. 3.—Turbulent velocity vs. phase for the two observing periods; see text for details

number 2.5 of the RR Lyrae survey computed by Stellingwerf (1975). This model has been used as a test case in the development and testing of a convection theory (Stellingwerf, 1982*a*, *b*, 1983, 1984*a*, *b*). The limiting amplitude behavior of this model is discussed in Stellingwerf (1984*c*). Although the model is not an exact match to the parameters of RR Lyrae (it is somewhat cooler and more luminous and has a longer period), the amplitude is correct, and it should suffice for a general comparison. The model parameters are:  $L = 2.46 \times 10^{35}$  ergs  $s^{-1}$ ,  $T_e = 6500$  K,  $M = 0.578 M_\odot$ ,  $X = 0.70$ ,  $Z = 0.001$ . The period of the fundamental mode of this model is 0.8 days, and the limiting amplitudes are:  $2K = 73.7$  km  $s^{-1}$ ,  $\delta M_{bol} = 0.747$ , and  $\delta R/R = 0.149$ . The observed velocity amplitude for RR Lyrae is 55 km  $s^{-1}$  in Figures 1*a* and 1*b*, implying a physical amplitude (including the geometrical correction) close to that of the model.

The behavior of the convective zone as a function of phase of pulsation is shown in Figure 8 of Stellingwerf (1984*c*). Several phases near minimum radius are reproduced here in somewhat greater detail as Figures 4*a*, 4*b*, 4*c*, and 4*d*. The constant 0.2 has been added to the phases here relative to the previous paper to agree with the observational phases in previous figures (phase zero is now maximum radius). The convection in this model is nearly constant for phases 0.2–0.425 (Fig. 4*a*), then exhibits a dramatic increase in strength at phase 0.47 (Fig. 4*b*), just preceding minimum radius at phase 0.525 (Fig. 4*c*). This is the strongest compressional phase of the pulsation in the outer layers, and convection carries all the energy flux over a broad region of the model including the hydrogen and helium ionization zones. Immediately following this period of increased turbulence, the model shows an even more dramatic decrease in the turbulent field parameters at phase 0.60 (Fig. 4*d*), at which time convection is virtually absent, carrying only 15% of the energy flux in the helium ionization zone, and 4% in the hydrogen zone. This behavior agrees with the phasing found in the observations, and is even more apparent in the (somewhat cleaner) Cepheid observations reported in Benz and Mayor

(1982) who specifically noted the rapid decline in the turbulent velocities following minimum radius. It will be shown in a separate paper (Stellingwerf 1985) that this phasing of the convective velocities can be understood in terms of a simple one-zone pulsation model. The simple model predicts that the turbulent velocities will vary in phase with the radial velocity for blue stars and inversely with the radius variation for red stars. In either case, maximum turbulence occurs near the phase of minimum radius, as seen here.

The velocities in Figure 4 are given in units of the sound speed and represent the rms width of the turbulent velocity distribution at a given time and mass level in the star. The sound speed is 16 km  $s^{-1}$  in the hydrogen zone (12,000 K), and 32 km  $s^{-1}$  in the second helium ionization zone (44,000 K). Peak rms velocities obtained in this model are thus about 5 km  $s^{-1}$  in the hydrogen zone (near the photosphere) and about 10 km  $s^{-1}$  in the second helium zone. These values are in qualitative agreement with the observed turbulent velocities shown in Figure 3.

Figure 5 shows the phase variation of the rms turbulent velocity at its peak value and at the outer zone of the model, as well as at various fixed temperature levels (*dashed lines*). The low values in the outer zone are caused by the outer convective boundary condition (zero velocity). This boundary condition also affects the fixed temperature curves, since the compressional heating near the phase of minimum radius causes a shift toward the surface of these curves.

Another effect also contributes to the line broadening: the gradient of the mean velocity field across the line-forming region. We estimate this effect by simply evaluating the change in the mean pulsation velocity from the surface of the model to a depth of  $\approx 10,000$  K. The result is plotted as the dotted line in Figure 5: it is a 1–2 km  $s^{-1}$  effect with a peak just preceding the increase in turbulence near  $R_{min}$ .

The CORAVEL instrument samples temperatures primarily in the range 5000–6000 K (Fe lines). Although the model turbulent velocities are only 1–3 km  $s^{-1}$  at this depth, there are two

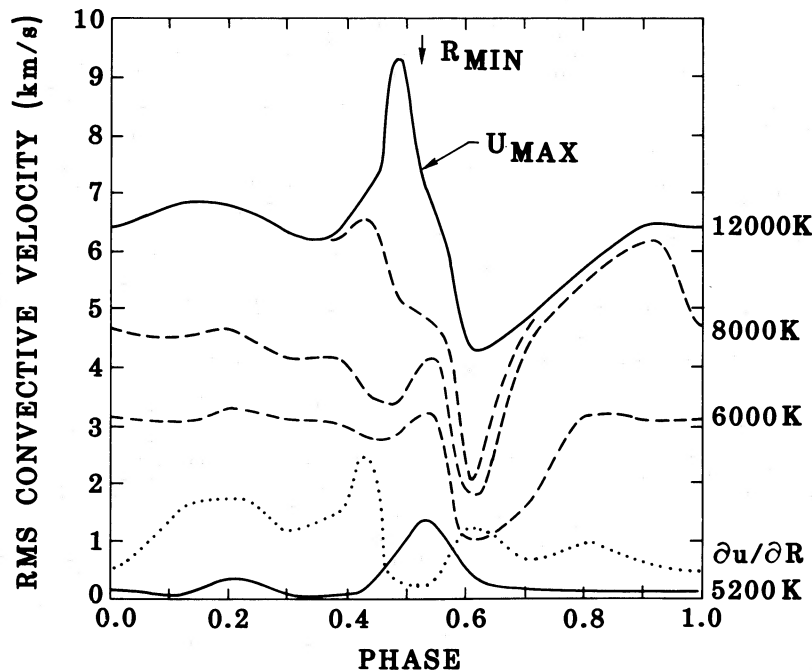


FIG. 4.—Model convective structure at four phases: *solid line*, turbulent rms velocity (units of sound speed); *dashed line*, convective luminosity (units of total luminosity).

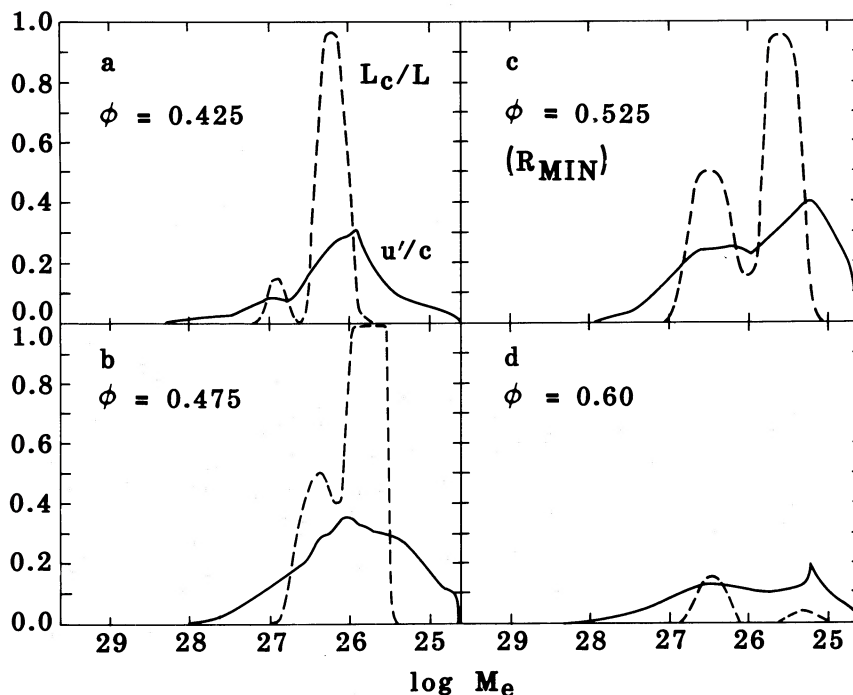


FIG. 5.—Model convective rms velocity vs. phase at various depths in the atmosphere. *Solid lines*: maximum convective velocity; *dashed lines*: velocities at constant temperatures; *dotted line*: effect of velocity gradients across the atmosphere.

reasons for comparing the observed turbulence to the model results at the hydrogen zone, rather than the surface: (1) the outer boundary condition undoubtedly suppresses the outermost turbulent velocities in the model, and (2) the temperature fluctuation because of the convection in the hydrogen zone reaches values of  $\delta T/T = 100\%$  at the phase of minimum radius; thus it is likely that 6000 K material exists with velocities near the peak turbulent velocities and that the spectrometer actually sees this high-velocity material from a deeper level than one might expect. It is also possible that part of the scatter seen in Figure 3 arises from convective structures that are changing on a short time scale, causing the line-forming region to occur at a variable depth in the atmosphere.

If the maximum convective velocities found in the model are compared with the maximum observed turbulent velocities at a given phase, the agreement is quite good, a remarkable result in view of the low signal-to-noise ratio level in the observations and the simplifications of the model.

#### V. DISCUSSION

In this paper we have shown that direct observation of the phase variation of the turbulence in RR Lyrae is possible, although not an easy task. The derived turbulent velocities show considerable scatter, at least part of which can be shown to be due to low contrast in the data analysis caused by the high effective temperature of RR Lyrae relative to the

CORAVEL standard (Arcturus). The highest velocities do show a relatively smooth envelope; however, peaking at about  $10 \text{ km s}^{-1}$  near the phase of minimum radius.

These observational results have been compared to a nonlinear pulsation model. The model includes a simple model of the turbulence, but one that takes into account the effects of overshooting, time dependence, coupling with pulsation, and nonlinearities. Insofar as comparison is possible, the model agrees with the observations, predicting both the correct phasing as well as the correct magnitude of the turbulence.

This preliminary look at the possibility of direct measurement of stellar turbulence using CORAVEL is encouraging. The detection of systematic differences between stars and between classes of variable stars may be attainable, with a strong possibility of theoretical explanation of the effect. As mentioned above, the data on Cepheids is less subject to observational scatter than the RR Lyrae data, so comparison with Cepheid models is planned as a follow-up to the present work.

We wish to warmly thank Dr. G. Burki from Geneva Observatory for making the observations during his observing period of 1983 October. This research was supported in part by the Swiss National Science Foundation and by NSF research grant AST-11029 through Mission Research Corporation and by a computational grant from Los Alamos National Laboratory.

#### REFERENCES

- Baranne, A., Mayor, M., and Poncet, J. L. 1979, *Vistas Astr.*, **23**, 279.  
 Benz, W., and Mayor, M. 1981, *Astr. Ap.*, **93**, 235.  
 ———. 1982, *Astr. Ap.*, **111**, 224.  
 ———. 1984, *Astr. Ap.*, **138**, 93.  
 Mayor, M. 1980, *Astr. Ap.*, **87**, L1.  
 Stellingwerf, R. F. 1975, *Ap. J.*, **195**, 441.  
 ———. 1982a, *Ap. J.*, **262**, 330.  
 Stellingwerf, R. F. 1982b, *Ap. J.*, **262**, 339.  
 ———. 1983, in *IAU Symposium 105, Observational Tests of the Stellar Evolution Theory*, ed. A. Maeder and A. Renzini (Dordrecht: Reidel), p. 461.  
 ———. 1984a, *Ap. J.*, **277**, 322.  
 ———. 1984b, *Ap. J.*, **277**, 327.  
 ———. 1984c, *Ap. J.*, **284**, 712.  
 ———. 1985, in preparation.

WILLY BENZ: Los Alamos National Laboratory, T-6 MS B288, Los Alamos, NM 87544

ROBERT F. STELLINGWERF: Mission Research Corporation, 1720 Randolph Road, S.E., Albuquerque, NM 87106